

Multiple climbing fibers signal to molecular layer interneurons exclusively via glutamate spillover

Germán Szapiro & Boris Barbour

Spillover of glutamate under physiological conditions has only been established as an adjunct to conventional synaptic transmission. Here we describe a pure spillover connection between the climbing fiber and molecular layer interneurons in the rat cerebellar cortex. We show that, instead of acting via conventional synapses, multiple climbing fibers activate AMPA- and NMDA-type glutamate receptors on interneurons exclusively via spillover. Spillover from the climbing fiber represents a form of glutamatergic volume transmission that could be triggered in a regionalized manner by experimentally observed synchronous climbing fiber activity. Climbing fibers are known to direct parallel fiber synaptic plasticity in interneurons, so one function of this spillover is likely to involve controlling synaptic plasticity.

Spillover of neurotransmitter—action at synaptic contacts other than those where it was released—has proved to be a controversial subject. For simple, small glutamatergic synapses, spillover has only rarely been reported^{1,2} at activity levels that are physiologically plausible, and modeling suggests that the spillover of glutamate at simple synapses is probably not significant³ (but see ref. 4). It has been argued that spillover would reduce synaptic independence and thus reduce the storage capacity of the brain³. However, the effect of spillover would not be disadvantageous at all synapses. In contrast to the many small synapses at which spillover is probably unimportant, a number of specialized synapses exist in the brain at which spillover has been clearly demonstrated and at which its functional role is apparent. These include the avian calyx of Held synapse⁵ and the cerebellar mossy fiber–granule cell synapse^{6,7}. However, these connections also mediate conventional synaptic transmission, and the role of spillover is essentially one of amplification: increasing the postsynaptic response to a given amount of transmitter. Physiological actions of spillover glutamate in the absence of conventional synaptic transmission have so far been restricted to glial cells^{8,9}.

Cerebellar climbing fibers constitute one of the two major afferent pathways to the cerebellum. They have a unique role in supervising motor learning, notably at the parallel fiber–Purkinje cell synapse in the cerebellar cortex. Beyond the well-characterized input to Purkinje cells, climbing fibers signal to glial cells via synaptic transmission¹⁰ and ectopic release¹¹. Anatomical studies have also mentioned the possibility of a climbing fiber–molecular layer interneuron synapse^{12,13}.

A climbing fiber input to molecular layer interneurons (stellate and basket cells) was recently identified^{14–16} and was shown to direct parallel fiber plasticity in these cells. However, the underlying synaptic mechanisms were not characterized beyond the initial current-clamp recordings. A notable twist in the study of this connection is the very recent demonstration that it is a prime example of a previously

unknown type of axodendritic (or axosomatic) contact¹⁷. Despite extensive and tight apposition between axonal (climbing fiber) and somatodendritic (interneuron) membranes, the apparent absence of vesicles and glutamate receptors argues against classical synaptic transmission occurring at these junctions.

Here we confirm the existence of the climbing fiber–interneuron connection and characterize its mechanism of transmission. We show that it is mediated exclusively by the spillover of glutamate and that multiple climbing fibers can influence a single interneuron. This spillover provides a mechanism allowing climbing fibers to signal to numerous synapses in a defined spatial region by a form of glutamatergic volume transmission.

RESULTS

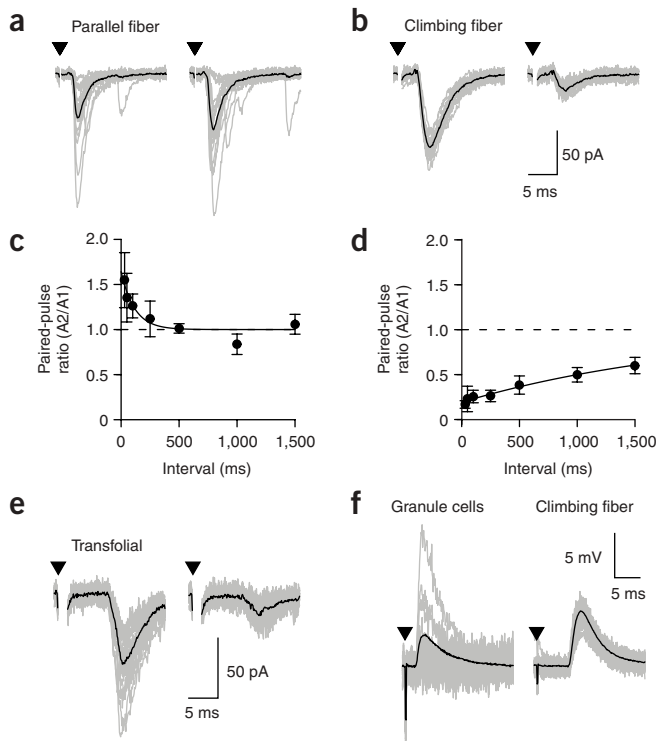
Climbing fiber inputs show paired-pulse depression

We made patch-clamp recordings from molecular layer interneurons (most of whose somata were near the Purkinje cell layer) in cerebellar slices. It was trivial to elicit rapid excitatory postsynaptic currents (EPSCs) that showed paired-pulse facilitation—representing granule cell inputs¹⁸ (**Fig. 1a**). The mean amplitude of the inputs we recorded was 249 ± 273 pA ($n = 20$; these are potentially compound responses). The 20–80% rise time was 0.41 ± 0.14 ms and the decay time constant was 1.85 ± 0.52 ms. More rarely, however, we were able to isolate inputs of a notably different nature, which showed marked paired-pulse depression (**Fig. 1b**). We considered these as putative climbing fiber inputs, as climbing fiber inputs to other cells depress similarly^{10,19}. They were all-or-none and had an average amplitude of 99 ± 94 pA ($n = 30$), a 20–80% rise time of 0.78 ± 0.27 ms and a decay time constant of 3.4 ± 1.4 ms. The rise times and decay time constants were significantly different from those of the parallel fiber inputs ($P < 10^{-7}$ for both parameters). Another difference between the two inputs was their variability, which was quantified by the coefficient of variation

Laboratoire de Neurobiologie, Ecole Normale Supérieure, CNRS, 46 rue d'Ulm, 75005 Paris, France. Correspondence should be addressed to B.B. (barbour@ens.fr).

Received 19 March; accepted 12 April; published online 21 May 2007; doi:10.1038/nn1907





(s.d./mean: 0.43 ± 0.23 , $n = 12$, for parallel fiber inputs; 0.20 ± 0.10 , $n = 12$, for climbing fiber inputs; $P = 0.005$) and the Fano factor (variance/mean: 32.3 ± 31.8 pA for parallel fiber inputs; 3.9 ± 2.7 pA for climbing fiber inputs; $P < 10^{-5}$). If both inputs were composed of the sum of identical independent random variants (for example, mEPSCs), but in different numbers (to explain the different amplitudes), they would still have the same Fano factor. Because climbing fiber inputs have a lower Fano factor than parallel fiber inputs do, this indicates that they are not composed of the same 'building blocks'.

The recordings here were carried out at $\sim 32^\circ\text{C}$. In four cells we compared responses at 32 and 37°C to confirm that the climbing fiber response was present at physiological temperatures (data not shown). At 37°C the amplitude of the response was reduced by $26 \pm 11\%$ and the 20–80% rise time was reduced by $16 \pm 15\%$, but the decay was unaffected. The latency was $15 \pm 8\%$ shorter.

The parallel fiber inputs recovered from facilitation with an average time constant of 116 ms (Fig. 1c), close to the values previously reported¹⁸ and as observed in Purkinje cells¹⁹. In contrast, the putative climbing fiber input showed a very slow recovery from depression ($\tau = 2.1$ s; Fig. 1d), which was strongly reminiscent of climbing fiber inputs to Purkinje cells¹⁹ and NG2⁺ glia¹⁰.

We further strengthened the identification of the climbing fiber input by stimulation in the molecular layer at distances > 600 μm from the interneuron, sometimes in neighboring folia: that is, transfolial stimulation. In sagittal slices, the only excitatory fiber whose branches show significant extent in the sagittal plane and also reach the molecular layer is the climbing fiber. At such distances, we were able to elicit depressing responses (Fig. 1e), and only such responses ($n = 4$). These presumably reflect the initiation of an action potential in one terminal branch and propagation to another branch contacting the recorded cell.

We next compared current-clamp responses for the two types of input (Fig. 1f). The parallel fiber input was elicited by juxta-threshold stimulation in the granule cell layer. The interneuron was maintained

Figure 1 Putative climbing fiber responses show paired-pulse depression. (a) A parallel fiber response shows paired-pulse facilitation (second amplitude/first amplitude, $A_2/A_1 = 1.27$, interval = 130 ms). Individual sweeps (gray) and the average (black, $n = 20$) are shown. In all figures, the times of stimulation are marked by triangles and the stimulus artifacts have usually been blanked. (b) A putative climbing fiber response shows marked paired-pulse depression ($A_2/A_1 = 0.25$, interval = 130 ms). Individual sweeps (gray) and the average (black, $n = 20$) are shown. (c) Recovery from paired-pulse facilitation for parallel fiber connections occurred with an average time constant of 116 ms and an intercept of 1.64 (mean \pm s.d., $n = 7$ cells). (d) Recovery from paired-pulse depression for putative climbing fiber inputs occurred with an average time constant of 2.1 s and an intercept of 0.19 ($n = 4$ – 7 cells). (e) Transfolial stimulation. A typical response recorded when stimulating in the distant molecular layer is shown (individual sweeps are gray and the average is black, $n = 22$). (f) Voltage recordings. Typical responses to juxta-threshold stimulation of granule cells (left, specimen traces in gray and the average of 100 in black) and a putative climbing fiber input in a different cell (right, specimen traces in gray and the average of 60 in black) are shown.

near -74 mV. We measured the kinetic properties of excitatory postsynaptic potentials (EPSPs) of the two inputs. For the parallel fiber ($n = 5$): mean amplitude 1.4 ± 1.2 mV, 20–80% rise time 0.66 ± 0.20 ms, decay time constant 4.8 ± 1.5 ms. For the climbing fiber ($n = 5$): mean amplitude 5.5 ± 2.5 mV, 20–80% rise time 1.2 ± 0.4 ms, decay time constant 6.9 ± 4.1 ms. The difference in rise times ($P = 0.05$; two-tailed t -test) was consistent with the previous description¹⁶.

We obtained final proof that the climbing fiber was the source of these depressing responses by recording from Purkinje cells and interneurons simultaneously and stimulating a common climbing fiber input (Fig. 2a). The EPSCs in both cells showed correlated all-or-none behavior as the stimulation intensity was varied around the threshold by a small amount (Fig. 2b), proving the commonality of the input to the two cells. Notably, the interneuron response was significantly delayed compared with the Purkinje cell response (Fig. 2c). The mean difference of the time to 5% rise was 0.83 ± 0.52 ms (interneuron succeeding the Purkinje cell; $P = 0.02$, $n = 7$), consistent with the previous report¹⁶.

Climbing fibers activate NMDA and AMPA receptors

We next characterized the postsynaptic receptors that mediate the climbing fiber response. Under control conditions, the EPSC was

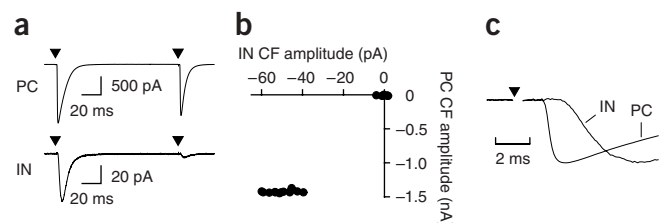


Figure 2 Purkinje cell and interneuron responses to common climbing fiber. (a) Climbing fiber (CF) responses in a simultaneously recorded Purkinje cell (top) and interneuron (bottom); averages of 35 sweeps (PC, Purkinje cell; IN, interneuron). Both cells were recorded with the cesium/TEA-based internal solution. The Purkinje cell was held at a depolarized potential to help inactivate voltage-dependent conductances. (b) Scatter plot of peak responses in the Purkinje cell and interneuron measured as the stimulus intensity was varied by a small fraction around threshold. The perfect correlation shows that the responses were caused by a single common input. (c) Same averages (first pulses) as in a, but scaled to the same peak amplitude to facilitate comparison of their time courses. The interneuron response had a markedly longer latency.

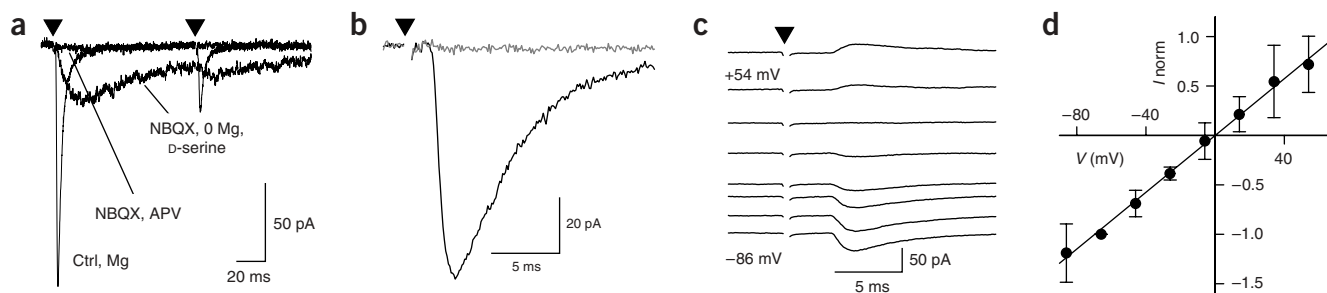


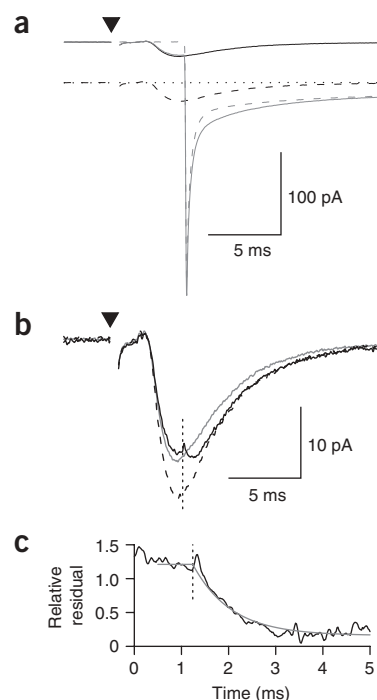
Figure 3 Climbing fiber inputs activate AMPA- and NMDA-type glutamate receptors. **(a)** The AMPA/kainate receptor-mediated component of the climbing fiber EPSC was isolated under control conditions (in the presence of Mg, which blocks NMDA receptors: Ctrl, Mg). The NMDA receptor-mediated component was isolated by application of 4 μ M NBQX and 45 μ M D-serine and nominal removal of Mg ions (NBQX, 0 Mg, D-serine). No response was detectable after addition of 50 μ M APV (NBQX, APV). Averages of 21 sweeps. **(b)** The sensitivity of the control response (black) to GYKI 53655 (gray; 50 μ M) indicated that no kainate receptors contributed to the non-NMDA receptor component. Averages of 41 traces. **(c)** Specimen traces showing the voltage dependence of the climbing fiber–interneuron response (using a cesium/TEA-based internal solution and recorded in the presence of bicuculline, but in the absence of muscimol). Traces were recorded at 20-mV intervals between -86 mV and $+54$ mV. Averages of 15 sweeps. **(d)** Pooled I - V data (mean \pm s.d., $n = 3$ –7 cells per point) for the EPSC peak normalized to the response at -66 mV, reflecting the AMPA receptor-mediated component. The average voltage dependence was linear with a reversal potential at zero.

blocked by 4 μ M 2,3-dihydroxy-6-nitro-7-sulfamoyl-benzo[*f*]quinoxaline-2,3-dione (NBQX) (**Fig. 3a**), indicating that the EPSC was mediated by AMPA/kainate receptors (mean kinetic parameters for this component were ($n = 5$) amplitude, 65 ± 31 pA; 20–80% rise time, 0.73 ± 0.11 ms; decay time constant, 3.11 ± 0.69 ms). The subsequent nominal removal of Mg from the solution (and addition of 45 μ M D-serine) always unmasked a slower component that was blocked by 50 μ M D-(–)-2-amino-5-phosphonovaleric acid, APV (**Fig. 3a**; mean kinetic parameters of this component were ($n = 5$) amplitude, 9.1 ± 8.3 pA; 20–80% rise time, 7.9 ± 3.6 ms; decay time constant, 98 ± 86 ms). The decay time constant was approximate, as the paired-pulse protocol used did not allow for the full decay of the NMDA component. In separate recordings, we confirmed the presence of an NMDA receptor-mediated outward current at $+54$ mV that was blocked by 50 μ M APV ($n = 4$; data not shown). We further analyzed the nature of the AMPA/kainate component with GYKI 53655, which abolished the control response in five cells, indicating that the response was a pure AMPA response and was not mediated by kainate receptors (**Fig. 3b**). Thus, climbing fibers activate NMDA receptors as well as AMPA-type glutamate receptors, in marked contrast to the parallel fiber input, which does not activate NMDA receptors under basal stimulation conditions²⁰.

Figure 4 The climbing fiber conductance is long lasting. **(a)** Current responses to the sequence of voltage jumps and synaptic stimulations required to test for the presence of an active synaptic conductance during the recorded EPSC time course (solid black, EPSC at -68 mV; dotted black, background current at -98 mV; dashed black, EPSC at -98 mV; dashed gray, jump from -68 mV to -98 mV in the absence of an EPSC; solid gray, jump shortly after the peak of the EPSC). Averages of ~ 50 sweeps. **(b)** The synaptic responses in **a** were separated from the capacity transients by subtraction, yielding the EPSC at -68 mV (solid gray), the EPSC at -98 mV (dashed black) and the test EPSC (solid black) subjected to a voltage jump (timing shown by dotted black line). When subjected to the voltage jump from -68 mV to -98 mV (timing indicated by the vertical dotted line), the EPSC rapidly approached that recorded at -98 mV, showing that the synaptic conductance was still active. **(c)** Plot of $[\text{EPSC}(-98 \text{ mV}) - \text{test EPSC}] / [\text{EPSC}(-98 \text{ mV}) - \text{EPSC}(-68 \text{ mV})]$ ('relative residual'; black). This indicates how quickly the test EPSC approached the EPSC at -98 mV. An exponential fit (gray) yielded a time constant of 0.81 ms. The offsets from 1 (before the jump) and 0 (at the end of the decay) probably represent errors caused by random variations in the averages, which are expected to be of a comparable magnitude.

We also investigated the voltage dependence of the climbing fiber response in interneurons (**Fig. 3c,d**). The EPSC peak current (AMPA component) showed a linear dependence on voltage and reversed at zero ($n = 3$ –7 cells), consistent with a nonspecific cation conductance, as is found in ionotropic glutamate receptors.

The response of the climbing fiber was significantly longer lasting than that of parallel fiber inputs (see above). This could reflect either a genuinely long-lasting synaptic conductance or a brief conductance in a cellular compartment subject to strong filtering, such as the axon. To distinguish between these two possibilities, we probed the time course of the underlying conductance by applying voltage jumps during the synaptic response. Our rationale was that only a conductance that is still active at the time of the jump will be affected by the change of driving force. A voltage jump rapidly changed the synaptic response, showing that the underlying synaptic conductance was genuinely



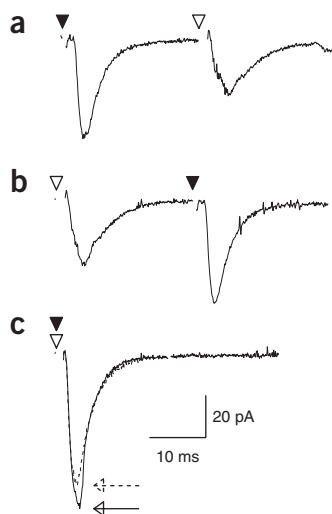


Figure 5 Interneurons are innervated by multiple climbing fibers. **(a)** Average responses ($n = 9$) of two putative climbing fiber inputs stimulated in succession. Both showed paired-pulse depression (data not shown). The filled and open triangles indicate the stimulus times for the two different stimulation electrodes. **(b)** The same two inputs were stimulated in reverse order. Note that each response has a similar amplitude as in **a**, indicating an absence of cross paired-pulse depression. Strong depression would have been expected if the same fiber were being stimulated twice (once by each stimulating electrode). **(c)** When stimulated simultaneously, the compound response (solid line and arrow) was clearly larger than either individual response. The compound response was slightly larger than the predicted sum of the individual responses (dashed line and arrow), but this difference was not significant on average (see text).

long lasting, rather than the result of filtering (Fig. 4). The speed of change can be characterized by a time constant (Fig. 4c) whose value was 1.1 ± 0.2 ms ($n = 4$). This appears consistent with a dendritic location, as the axon is expected to be poorly clamped and thus introduce stronger filtering.

Multiple climbing fibers contact a single interneuron

In the adult, most Purkinje cells are contacted by a single climbing fiber input. However, this one-to-one relation is not found at the climbing fiber connection on NG2⁺ glia¹⁰. We investigated whether interneurons

might receive input from multiple climbing fibers by searching for two inputs with different stimulating electrodes. It often proved possible to isolate two inputs of different amplitudes, both showing paired-pulse depression. In seven out of eight cases, these inputs did not interact via paired-pulse depression (Fig. 5a,b). The cell in which crossed paired-pulse depression appeared to occur was eliminated from further analysis, because a common climbing fiber was probably excited by the two stimulating electrodes. When stimulated simultaneously, the remaining putative pairs of climbing fiber inputs all summed to compound responses that were clearly larger than the individual responses (Fig. 5c). This could not have occurred if the two stimulating electrodes were exciting the same fiber, proving that at least two climbing fibers were signaling to each interneuron. The compound responses were on average slightly larger than the predicted sum of isolated responses ($6.5 \pm 12\%$ greater), but this difference was not significant ($P = 0.6$).

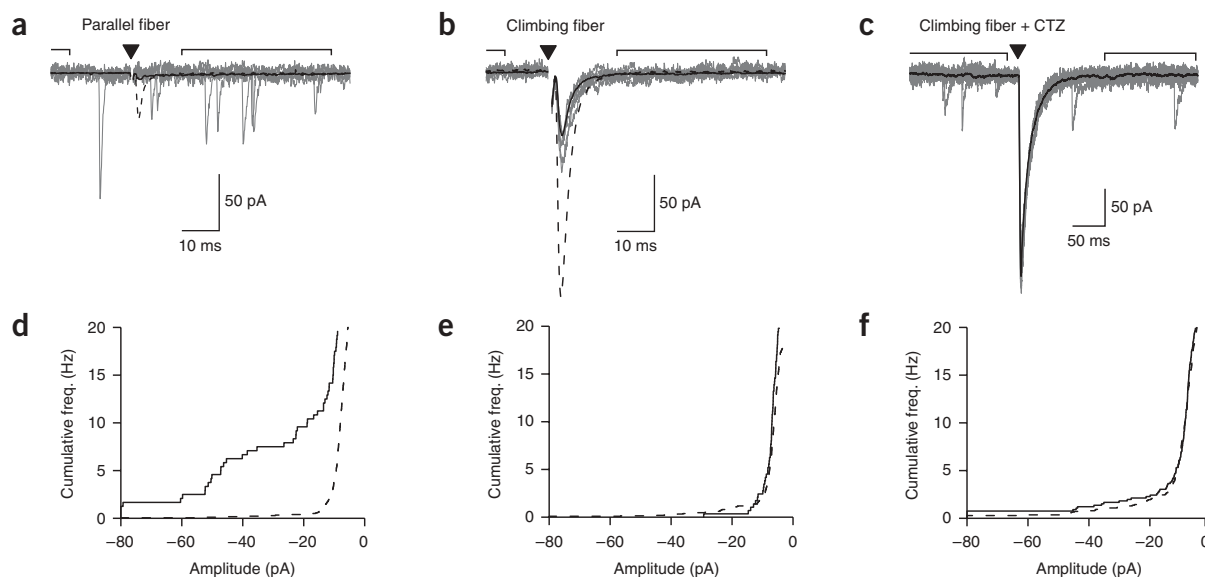


Figure 6 mEPSCs of the climbing fiber could not be detected. **(a)** Average responses of a parallel fiber input in control conditions (dashed black, $n = 100$) and in 5 mM strontium with nominally zero extracellular Ca (5 mM strontium/0 Ca, solid black, $n = 100$). Typical specimen sweeps in 5 mM strontium/0 Ca (gray) showed the presence of asynchronous mEPSCs. The horizontal brackets above the traces delimit the end of the prestimulus control period (left) and the poststimulus period (right), during which spontaneous EPSCs and evoked asynchronous mEPSCs were detected, respectively. **(b)** Same experiment as in **a**, but involving a climbing fiber input (the averages are of 30 and 90 traces, respectively). Note the apparent absence of evoked asynchronous mEPSCs in 5 mM strontium/0 Ca (gray specimen sweeps). **(c)** Similar experiment to **b**, but in the presence of cyclothiazide (CTZ, 100 μ M). Average response is black and individual traces gray. **(d)** Cumulative frequency distribution of EPSCs detected above a threshold of 5 pA before (dashed) and after parallel fiber stimulation (solid). The upstroke around 10 pA reflects the detection level at which noise began to trigger significant numbers of false positives. A clear excess of EPSCs greater than 10 pA ($P = 10^{-11}$), reflecting evoked asynchronous mEPSCs, was apparent following the stimulus. **(e)** Cumulative frequency plot as in **d**, but for the climbing fiber input of **b**. There was no significant difference ($P = 0.51$) in EPSC detection before and after the stimulus. **(f)** Cumulative frequency plot for the climbing fiber/cyclothiazide experiment of **c**. The rate of EPSC detection was not significantly different before and after stimulation ($P = 0.72$).

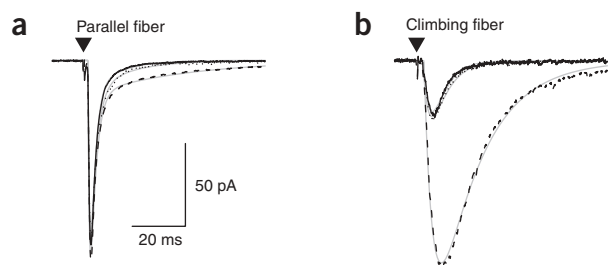


Figure 7 Blocking glutamate uptake potentiates the climbing fiber input. **(a)** The glutamate uptake blocker TBOA (50 μ M) had little effect on a parallel fiber input, mostly unmasking a small slow component (control, solid; TBOA, dashed; recovery, dotted). Exponential fits (see text) are shown in gray. Averages of 70, 80 and 19 sweeps, respectively. **(b)** TBOA had a strong effect on a climbing fiber response, potentiating and prolonging the entire EPSC. Same key as in **a**. Averages of 20, 30 and 21 sweeps, respectively.

Climbing fiber miniature EPSCs were undetectable

We then investigated the mechanisms underlying the low variability of the climbing fiber response. Because most synaptic variability is thought to arise from variations in the numbers of transmitter quanta released, we sought to determine the quantal properties of the connections of granule cells and climbing fibers to interneurons.

A sensitive method for detecting and measuring quantal events is to record asynchronous miniature EPSCs following stimulation in the presence of strontium ions^{21,22}. This method can resolve mEPSCs released by the climbing fiber onto other cell types^{10,11,23,24}. We carried out this experiment on parallel fiber and climbing fiber inputs (Fig. 6). Nominal removal of extracellular calcium ions and the addition of 5 mM strontium caused a large reduction of the phasic response and the appearance of spontaneous mEPSCs in the period following the stimulation (that is, tens of milliseconds) (Fig. 6a, responses to stimulation of what was probably a single granule cell input). Climbing fiber connections showed quite different behavior from parallel fibers in strontium; no asynchronous mEPSCs were apparent (Fig. 6b).

To quantify the frequencies of mEPSC occurrence in the presence of strontium ions, it was necessary to take into account the fact that spontaneous (m)EPSCs, mostly arising at other synapses, are observed at a low rate in interneurons. We therefore compared the rates of EPSC detection within defined windows before (–311 to –16 ms) and after (14 to 54 ms) stimulation. EPSCs were detected and measured automatically (see Methods and Fig. 6). The detection of mEPSCs was limited by the recording noise, which gave rise to an increasing number of false positives as the detection threshold was lowered below ≈ 10 pA. We therefore tested the significance of the different rates of mEPSC detection above a threshold amplitude of 10 pA, before and after stimulation, using the statistical test described in the Methods (which enabled us to evaluate the significance individually for each connection). For each parallel fiber connection tested ($n = 4$), the rate of mEPSC detection after stimulation (mean 12.3 ± 4.5 Hz) was significantly greater than before (mean 2.1 ± 1.4 Hz; $P < 10^{-4}$ in all cases) (Fig. 6d). The increased rate of mEPSC detection after the stimulus is a result of the action of strontium, and does not reflect normal ‘delayed release’²⁵, as the poststimulus detection rate under control conditions (2.3 ± 0.8 Hz, $n = 3$) was similar to the prestimulus rate in the same conditions (1.8 ± 0.9 Hz), and much lower than the poststimulus detection rates in strontium. In marked contrast to the behavior of the parallel fiber synapse in strontium, for all climbing fiber connections, the mEPSC detection rates before and after stimulation

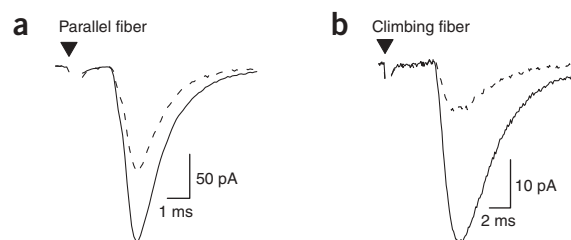


Figure 8 The climbing fiber input is highly sensitive to block by low-affinity AMPA receptor antagonists. **(a)** Average parallel fiber responses ($n = 30$) in the absence (solid) and presence (dashed) of DGG (0.375 mM). **(b)** Average climbing fiber responses ($n = 30$) in the absence (solid) and presence (dashed) of DGG (0.375 mM). The climbing fiber response was blocked by the DGG to a greater degree than was the parallel fiber input.

were not significantly different ($n = 8$, P range 0.06–1; an example is shown in Fig. 6e).

We also carried out a similar experiment for the climbing fiber input in the presence of cyclothiazide (CTZ, 100 μ M), to enhance mEPSCs that were potentially below the detection threshold. Although CTZ potentiated and prolonged the evoked climbing fiber response in strontium, we were still unable to detect any excess of mEPSCs after climbing fiber stimulation ($n = 4$, 47–120 sweeps, $P = 0.07$ –0.83) (Fig. 6c,f). To avoid detection bias caused by the longer decay phase of the evoked EPSC in the presence of CTZ and strontium (the bias could result from noise or the slope), we carried out the detection in a time window 134–274 ms after stimulation. In all other climbing fiber connections studied in this way, mEPSCs were detected at these times^{10,11,23,24}.

Thus, we could not detect mEPSCs of the climbing fiber–interneuron connection, suggesting that glutamate is not liberated directly opposite significant densities of receptors on the interneuron.

Strong potentiation by glutamate uptake block

We next performed experiments designed to test whether it was necessary for glutamate to diffuse a significant distance after its release to reach the interneuron. It is well established, both experimentally and theoretically, that spillover responses are selectively reduced by the action of uptake^{1,3,4,26–30}.

We applied DL-threo- β -benzyloxyaspartate, TBOA (50 μ M), a non-transported blocker of glutamate uptake, while recording parallel and climbing fiber responses. As expected, the effect on the parallel fiber response was minimal (Fig. 7a), with only a small, slow component of the response being affected²⁶. Fitting the time course of the parallel fiber EPSC in TBOA sometimes required three exponential components (one for the onset and two for the decay). The fit parameter values in control conditions were $A_1 = 414 \pm 247$ pA, $A_2 = -395 \pm 239$ pA, $A_3 = -19 \pm 12$ pA, $\tau_1 = 0.51 \pm 0.16$ ms, $\tau_2 = 1.40 \pm 0.37$ ms and $\tau_3 = 11.46 \pm 7.49$ ms ($n = 4$). In the presence of TBOA, these parameters were altered by less than 10%, except for A_3 (2.41 ± 2.66 fold change, $P = 0.37$, paired two-tailed Student’s t -test) and τ_3 (2.63 ± 0.91 fold change, $P = 0.04$, paired two-tailed Student’s t -test). The EPSC peak increased by $6 \pm 15\%$ in TBOA ($P = 0.47$, paired two-tailed Student’s t -test).

In marked contrast to the parallel fiber EPSC, the climbing fiber response was strongly enhanced and prolonged by TBOA (Fig. 7b). Its time course was satisfactorily fit by two exponentials (control values of amplitude, 49 ± 22 pA; onset time constant, 1.2 ± 0.7 ms; decay time constant, 4.2 ± 0.8 ms; $n = 6$). In TBOA, the amplitude was increased 2.6 ± 2.19 fold ($n = 6$, $P = 0.03$), and both the onset time constant

(3.13 ± 0.45 fold increase, $P = 0.03$) and the decay time constant (4.44 ± 1.57 fold increase, $P = 0.03$) were prolonged.

This sensitivity to uptake block suggests that glutamate from the climbing fiber diffuses a significant distance before reaching the interneuron, which would allow its concentration to be strongly reduced by uptake. The effect of TBOA also rules out the possibility that the EPSCs we recorded involved reversed glutamate uptake releasing glutamate into the extracellular space, or that forward glutamate uptake generated the EPSCs in the interneuron, as both forward and backward glutamate uptake are blocked by TBOA^{31,32}.

Strong inhibition by low-affinity AMPA receptor antagonist

The degree of inhibition of glutamate receptors by low-affinity competitive antagonists depends (at equilibrium) on the competing concentration of glutamate, which yields information about the glutamate concentration underlying synaptic responses³³. If the climbing fiber response results from glutamate spillover, it would be expected to involve lower glutamate concentrations than standard synaptic transmission and therefore be particularly sensitive to blocking by such antagonists.

We applied the low-affinity antagonist of AMPA/kainate-type glutamate receptors γ -D-glutamyl-glycine (DGG) at 0.375 mM to parallel and climbing fiber inputs (Fig. 8). DGG blocked the parallel fiber inputs by $39 \pm 11\%$ ($n = 5$), whereas it blocked the climbing fiber response by $72 \pm 7\%$ ($n = 6$). The difference was significant ($P = 0.004$) and thus suggests that during the climbing fiber response receptors are exposed to a lower concentration of glutamate than they are during the parallel fiber response. The sensitivity of the climbing fiber response to DGG in interneurons further supports the notion that the EPSC is elicited by glutamate spillover.

DISCUSSION

Spillover from climbing fibers to interneurons

We have characterized the climbing fiber–molecular layer interneuron input. It has strong and long-lasting paired-pulse depression and has both AMPA and NMDA receptor–dependent components. Multiple climbing fibers probably signal to each interneuron. The climbing fiber to interneuron connection shows a number of unusual properties: in particular, the absence of detectable mEPSCs, the invariance of response amplitudes and the sensitivity to uptake block. These led us to consider three different mechanisms of synaptic signaling: standard transmission, ectopic release and spillover.

Our inability to detect mEPSCs suggests that transmitter release does not occur opposite any significant densities of glutamate receptors, thus arguing against both standard synaptic transmission and ectopic release. The absence of detectable mEPSCs is, however, consistent with a spillover mechanism, as the response could result from the interaction of many vesicles released from a large area of the climbing fiber, while individually each vesicle only produces a much attenuated response in the interneuron. The strong potentiation by uptake blockers indicates that receptors are reached only after the transmitter has diffused some distance. This again argues in favor of spillover and against both standard transmission and ectopic release.

Further support for the spillover mechanism is provided by the strong block of the climbing fiber–interneuron response by DGG; other cerebellar synaptic responses^{24,34}, including spillover responses³⁵, are less inhibited by higher DGG concentrations. A difference in the amount of block between direct synaptic and spillover responses similar to that shown here has been observed at the cerebellar mossy fiber–granule cell synapse using a different low-affinity antagonist (kynurenate)⁶.

Finally, recent electron microscopy of the climbing fiber–interneuron apposition¹⁷ argues strongly against both a standard synapse and ectopic release, as the authors were unable to detect significant densities of vesicles or glutamate receptors (either AMPA or NMDA types) at the junctions. Moreover, by demonstrating such a close approach of the climbing fiber to the interneuron dendrite, the report also provides indirect support for the spillover hypothesis, as the action of spillover glutamate is strongest over short distances³. Our data provide no insight into the function of the potassium channel clusters found at the climbing fiber–interneuron appositions.

We conclude, therefore, that climbing fiber–interneuron signaling occurs via spillover. However, the relative contributions of spillover from release onto Purkinje cells, NG2⁺ cells and Bergmann glia (including ectopic release) are unknown.

Comparison with previous reports

Although we did not keep detailed records, we estimate that a climbing fiber connection could be found in a majority of the interneurons tested. We also estimate that multiple inputs are frequent. This fits with the previous report¹⁶ that all stellate and basket cells received climbing fiber inputs.

Our results agree closely with the *in vivo* observations¹⁶ in other respects, including the slower kinetics of the climbing fiber than parallel fiber responses, and the delay between the responses in Purkinje cells and interneurons, which presumably reflects a combination of conduction, diffusion and receptor activation delays.

It has been reported that high-frequency (5–50 Hz) activation of climbing fibers caused a reduction of interneuronal inhibition recorded in Purkinje cells, via an action on AMPA receptors on the interneuron axon^{36–38}. The question arises of whether the EPSC reported here is linked to their effect. However, the properties reported by those authors show significant discrepancies with those we found. In particular, instead of high-frequency signaling to the axon, the EPSC we recorded seems to mediate low-frequency signaling (because of the strong paired-pulse depression) to AMPA receptors on the dendrites of the interneuron (as suggested by the voltage jumps in Fig. 4). Moreover, although there is evidence for the expression of functional NMDA receptors on interneuron axons^{39–41}, only NMDA receptors on the dendrite are able to generate a current that is detectable from the soma²⁰.

Roles in network activity and synaptic plasticity

The climbing fiber input to interneurons is excitatory. If several inputs from synchronous climbing fibers combine to excite individual interneurons strongly, synchronous activation of interneurons within a sagittal band might be expected, as this is the typical pattern of correlated climbing fibers⁴². What would be the consequences of synchronous activation of interneurons? They inhibit most cells extending into the molecular layer, including the Purkinje cell. This inhibition would succeed the direct climbing fiber input to the Purkinje cell and may help to truncate the complex spike. An intriguing idea is that this inhibition might also be responsible for the pause in Purkinje cell simple spike activity that is often observed after complex spikes^{43,44}.

A role for the climbing fiber in controlling parallel fiber–interneuron synaptic plasticity has been reported^{15,16}. When parallel fibers are stimulated alone at a high frequency *in vivo*, no change of efficacy is observed. However, the same stimulation in conjunction with climbing fiber activity leads to a long-term potentiation. It seems unlikely that even multiple climbing fiber inputs would induce an electrical response that could be reliably distinguished from that of high-frequency parallel

fiber activity. This raises the question of how the climbing fiber generates a distinctive induction signal. The activation of NMDA receptors by the climbing fiber and subsequent calcium entry could represent an essentially nonelectrical signal that might distinguish climbing fiber from parallel fiber inputs, which have only been shown to activate NMDA receptors when stimulated in compact bundles, and not under basal stimulation conditions²⁰. Notably, NMDA receptor activation is necessary for⁴⁵, or can influence⁴⁶, the induction of long-term potentiation in the interneuron (studied *in vitro* without the climbing fiber).

Beyond the input to interneurons that we demonstrate here, it seems plausible that glutamate spillover may reach other cells in the molecular layer in a similar way; climbing fiber responses have been reported in Lugaro and Golgi cells, for instance (Ekerot, C. and Jörntell, H., *Abstract Viewer/Itinerary Planner*. Washington, DC: Society for Neuroscience 274.3, 2003), though it is not known whether they are also mediated by spillover. The climbing fiber may therefore provide a form of regionalized glutamatergic volume transmission that reaches many cells with dendrites in the molecular layer. This signaling could subservise both developmental and physiological roles.

METHODS

Animal preparation. Animal experimentation methods complied with French, European and US National Institutes of Health guidelines. Young male Wistar rats (postnatal day 17–25) were killed by decapitation and the cerebellum rapidly dissected into a cold low-sodium saline containing 230 mM sucrose, 26 mM NaHCO₃, 3 mM KCl, 1.25 mM NaH₂PO₄, 0.8 mM CaCl₂, 8 mM MgCl₂ and 25 mM D-glucose, bubbled with 95% CO₂/5% O₂ and supplemented with 50 μM D-APV. Sagittal and transverse slices 360 μm thick were cut in the same solution, using a Microm HM650V slicer. Slices recovered for 60 min in standard extracellular saline at 33 °C, containing 135 mM NaCl, 26 mM NaHCO₃, 3 mM KCl, 1.25 mM NaH₂PO₄, 2 mM CaCl₂, 1 mM MgCl₂ and 25 mM D-glucose, bubbled with 95% CO₂/5% O₂. Thereafter, the slices were stored at 20–26 °C.

Electrophysiology. Whole-cell voltage-clamp and current-clamp recordings were obtained at 30–33 °C from molecular layer interneurons using a Cairn Optopatch. Cells were usually clamped to –66 mV. One of two internal solutions was used, a potassium-gluconate-based internal or a cesium/tetraethylammonium (TEA)-methanesulfonate-based internal. The composition of the potassium-gluconate internal solution was 130 mM potassium gluconate, 10 mM KCl, 10 mM HEPES, 1 mM MgCl₂, 16 mM sucrose, 5 mM BAPTA, 4 mM Na₂ATP and 1 mM NaGTP, titrated to pH 7.3 with KOH. The cesium-methanesulfonate internal solution contained 135 mM CsCH₃O₃S, 5 mM TEA-Cl, 10 mM HEPES, 1 mM MgCl₂, 16 mM sucrose, 5 mM BAPTA, 4 mM Na₂ATP, 1 mM NaGTP and 10 mM QX-314, titrated to pH 7.3 with CsOH. Voltages were corrected for the junction potentials by –8 mV and –6 mV, respectively (measured at 32 °C). The external solution contained 10 μM bicuculline methochloride and 4–5 μM muscimol; the combination occluded GABAergic synaptic currents, but also induced a small tonic inhibitory conductance that reduced activity in coupled interneurons, which would otherwise have interfered with the recordings. Cyclothiazide was diluted from a 100 mM stock in DMSO. Chemicals and drugs were obtained from Sigma and Tocris. An isolated stimulator was connected to a saline-filled patch electrode; the stimulation frequency for recording was 0.1 Hz. Data were acquired using PClamp software (Molecular Dynamics) and analyzed within the Igor (Wave-metrics) graphical analysis environment.

Statistics. Where responses were fitted by exponentials, rising and decay phases were fitted simultaneously. The onset phase was always represented by a single exponential, whereas the decay phase was fitted with one or two components. The sum of the exponential amplitudes was constrained to be zero at the time of response onset (also fitted), to ensure its return to the baseline.

Unless otherwise stated, means and s.d. are given in the text and significance was tested using the nonparametric Wilcoxon signed rank test (two-tailed). Some statistical analysis was performed using GNU R (R Foundation for Statistical Computing). In particular, the statistical test for comparing two Poisson rates follows the description given in chapter 9 of ref. 47. This requires summation of a binomial distribution, for which the exact binomial test (binom.test) in GNU R was used.

ACKNOWLEDGMENTS

We thank H. Jörntell for help in identifying the climbing fiber input to interneurons; D. Colquhoun and A. Hawkes for showing us the test for comparing two Poisson rates; C. Mulle for the gift of GYKI 53655 and advice; D. Attwell, T. Otis and D. DiGregorio for comments on the manuscript; and C. Léna, A. Feltz, Y. Otsu and many other members of the Laboratoire de Neurobiologie for helpful discussion and comments on the manuscript. We gratefully acknowledge the support of the Agence Nationale de la Recherche, Fondation Fyssen (fellowship to G.S.), Centre National de la Recherche Scientifique and Ecole Normale Supérieure.

COMPETING INTERESTS STATEMENT

The authors declare no competing financial interests.

Published online at <http://www.nature.com/natureneuroscience>

Reprints and permissions information is available online at <http://npg.nature.com/reprintsandpermissions>

- Arnth-Jensen, N., Jabaudon, D. & Scanziani, M. Cooperation between independent hippocampal synapses is controlled by glutamate uptake. *Nat. Neurosci.* **5**, 325–331 (2002).
- Isaacson, J.S. Glutamate spillover mediates excitatory transmission in the rat olfactory bulb. *Neuron* **23**, 377–384 (1999).
- Barbour, B. An evaluation of synapse independence. *J. Neurosci.* **21**, 7969–7984 (2001).
- Rusakov, D.A. & Kullmann, D.M. Extrasynaptic glutamate diffusion in the hippocampus: ultrastructural constraints, uptake and receptor activation. *J. Neurosci.* **18**, 3158–3170 (1998).
- Trussell, L.O., Zhang, S. & Raman, I.M. Desensitization of AMPA receptors upon multiquantal neurotransmitter release. *Neuron* **10**, 1185–1196 (1993).
- DiGregorio, D.A., Nusser, Z. & Silver, R.A. Spillover of glutamate onto synaptic AMPA receptors enhances fast transmission at a cerebellar synapse. *Neuron* **35**, 521–533 (2002).
- Nielsen, T.A., DiGregorio, D.A. & Silver, R.A. Modulation of glutamate mobility reveals the mechanism underlying slow-rising AMPAR EPSCs and the diffusion coefficient in the synaptic cleft. *Neuron* **42**, 757–771 (2004).
- Clark, B.A. & Barbour, B. Currents evoked in Bergmann glial cells by parallel fibre stimulation in rat cerebellar slices. *J. Physiol. (Lond.)* **502**, 335–350 (1997).
- Bergles, D.E. & Jahr, C.E. Synaptic activation of glutamate transporters in hippocampal astrocytes. *Neuron* **19**, 1297–1308 (1997).
- Lin, S.C. *et al.* Climbing fiber innervation of NG2-expressing glia in the mammalian cerebellum. *Neuron* **46**, 773–785 (2005).
- Matsui, K. & Jahr, C.E. Ectopic release of synaptic vesicles. *Neuron* **40**, 1173–1183 (2003).
- Palay, S.L. & Chan-Palay, V. *Cerebellar Cortex* (Springer, New York, 1974).
- Sugihara, I., Wu, H. & Shinoda, Y. Morphology of single olivocerebellar axons labeled with biotinylated dextran amine in the rat. *J. Comp. Neurol.* **414**, 131–148 (1999).
- Ekerot, C.F. & Jörntell, H. Parallel fibre receptive fields of Purkinje cells and interneurons are climbing fibre-specific. *Eur. J. Neurosci.* **13**, 1303–1310 (2001).
- Jörntell, H. & Ekerot, C.F. Reciprocal bidirectional plasticity of parallel fibre receptive fields in cerebellar Purkinje cells and their afferent interneurons. *Neuron* **34**, 797–806 (2002).
- Jörntell, H. & Ekerot, C.F. Receptive field plasticity profoundly alters the cutaneous parallel fibre synaptic input to cerebellar interneurons *in vivo*. *J. Neurosci.* **23**, 9620–9631 (2003).
- Kollo, M., Holderith, N.B. & Nusser, Z. Novel subcellular distribution pattern of A-type K⁺ channels on neuronal surface. *J. Neurosci.* **26**, 2684–2691 (2006).
- Xu-Friedman, M.A. & Regehr, W.G. Probing fundamental aspects of synaptic transmission with strontium. *J. Neurosci.* **20**, 4414–4422 (2000).
- Konnerth, A., Llano, I. & Armstrong, C.M. Synaptic currents in cerebellar Purkinje cells. *Proc. Natl. Acad. Sci. USA* **87**, 2662–2665 (1990).
- Clark, B.A. & Cull-Candy, S.G. Activity-dependent recruitment of extrasynaptic NMDA receptor activation at an AMPA receptor-only synapse. *J. Neurosci.* **22**, 4428–4436 (2002).
- Dodge, F.A., Miledi, R. & Rahamimoff, R. Strontium and quantal release of transmitter at the neuromuscular junction. *J. Physiol. (Lond.)* **200**, 267–283 (1969).
- Xu-Friedman, M.A. & Regehr, W.G. Presynaptic strontium dynamics and synaptic transmission. *Biophys. J.* **76**, 2029–2042 (1999).
- Silver, R.A., Momiya, A. & Cull-Candy, S.G. Locus of frequency-dependent depression identified with multiple-probability fluctuation analysis at rat climbing fibre-Purkinje cell synapses. *J. Physiol. (Lond.)* **510**, 881–902 (1998).

24. Foster, K.A. & Regehr, W.G. Variance-mean analysis in the presence of a rapid antagonist indicates vesicle depletion underlies depression at the climbing fiber synapse. *Neuron* **43**, 119–131 (2004).
25. Atluri, P.P. & Regehr, W.G. Delayed release of neurotransmitter from cerebellar granule cells. *J. Neurosci.* **18**, 8214–8227 (1998).
26. Barbour, B., Keller, B.U., Llano, I. & Marty, A. Prolonged presence of glutamate during excitatory synaptic transmission to cerebellar Purkinje cells. *Neuron* **12**, 1331–1343 (1994).
27. Brasnjo, G. & Otis, T.S. Neuronal glutamate transporters control activation of post-synaptic metabotropic glutamate receptors and influence cerebellar long-term depression. *Neuron* **31**, 607–616 (2001).
28. Diamond, J.S. Neuronal glutamate transporters limit activation of NMDA receptors by neurotransmitter spillover on CA1 pyramidal cells. *J. Neurosci.* **21**, 8328–8338 (2001).
29. Marcaggi, P., Billups, D. & Attwell, D. The role of glial glutamate transporters in maintaining the independent operation of juvenile mouse cerebellar parallel fibre synapses. *J. Physiol. (Lond.)* **552**, 89–107 (2003).
30. Marcaggi, P. & Attwell, D. Endocannabinoid signaling depends on the spatial pattern of synapse activation. *Nat. Neurosci.* **8**, 776–781 (2005).
31. Marcaggi, P., Hirji, N. & Attwell, D. Release of L-aspartate by reversal of glutamate transporters. *Neuropharmacology* **49**, 843–849 (2005).
32. Owe, S.G., Marcaggi, P. & Attwell, D. The ionic stoichiometry of the GLAST glutamate transporter in salamander retinal glia. *J. Physiol. (Lond.)* **577**, 591–599 (2006).
33. Clements, J.D., Lester, R.A., Tong, G., Jahr, C.E. & Westbrook, G.L. The time course of glutamate in the synaptic cleft. *Science* **258**, 1498–1501 (1992).
34. Wadiche, J.I. & Jahr, C.E. Multivesicular release at climbing fiber–Purkinje cell synapses. *Neuron* **32**, 301–313 (2001).
35. Takayasu, Y., Iino, M., Shimamoto, K., Tanaka, K. & Ozawa, S. Glial glutamate transporters maintain one-to-one relationship at the climbing fiber–Purkinje cell synapse by preventing glutamate spillover. *J. Neurosci.* **26**, 6563–6572 (2006).
36. Satake, S., Saitow, F., Yamada, J. & Konishi, S. Synaptic activation of AMPA receptors inhibits GABA release from cerebellar interneurons. *Nat. Neurosci.* **3**, 551–558 (2000).
37. Satake, S., Saitow, F., Rusakov, D. & Konishi, S. AMPA receptor-mediated presynaptic inhibition at cerebellar GABAergic synapses: a characterization of molecular mechanisms. *Eur. J. Neurosci.* **19**, 2464–2474 (2004).
38. Satake, S. *et al.* Characterization of AMPA receptors targeted by the climbing fiber transmitter mediating presynaptic inhibition of GABAergic transmission at cerebellar interneuron–Purkinje cell synapses. *J. Neurosci.* **26**, 2278–2289 (2006).
39. Glitsch, M. & Marty, A. Presynaptic effects of NMDA in cerebellar Purkinje cells and interneurons. *J. Neurosci.* **19**, 511–519 (1999).
40. Duguid, I.C. & Smart, T.G. Retrograde activation of presynaptic NMDA receptors enhances GABA release at cerebellar interneuron–Purkinje cell synapses. *Nat. Neurosci.* **7**, 525–533 (2004).
41. Beierlein, M. & Regehr, W.G. Local interneurons regulate synaptic strength by retrograde release of endocannabinoids. *J. Neurosci.* **26**, 9935–9943 (2006).
42. Lang, E.J., Sugihara, I., Welsh, J.P. & Llinas, R. Patterns of spontaneous Purkinje cell complex spike activity in the awake rat. *J. Neurosci.* **19**, 2728–2739 (1999).
43. Granit, R. & Phillips, C.G. Excitatory and inhibitory processes acting upon individual Purkinje cells of the cerebellum in cats. *J. Physiol. (Lond.)* **133**, 520–547 (1956).
44. Sato, Y., Miura, A., Fushiki, H. & Kawasaki, T. Short-term modulation of cerebellar Purkinje cell activity after spontaneous climbing fiber input. *J. Neurophysiol.* **68**, 2051–2062 (1992).
45. Smith, S.L. & Otis, T.S. Pattern-dependent, simultaneous plasticity differentially transforms the input-output relationship of a feedforward circuit. *Proc. Natl. Acad. Sci. USA* **102**, 14901–14906 (2005).
46. Rancillac, A. & Crepel, F. Synapses between parallel fibres and stellate cells express long-term changes in synaptic efficacy in rat cerebellum. *J. Physiol. (Lond.)* **554**, 707–720 (2004).
47. Cox, D.R. & Lewis, P.A.W.L. *The Statistical Analysis of Series of Events* (Chapman & Hall, London, 1966).